December, 1983] © 1983 *The Chemical Society of Japan* *Bull. Chem. Soc. Jpn.*, **56**, *3635—3641 (1983)* 3635

An X-Ray Diffraction Study on the Structures of Mono(glycinato)nickel(II) and Tris(glycinato)nickelate(II) Complexes in Aqueous Solution

Kazuhiko Ozutsumi and Hitoshi Ohtaki*
Department of Electronic Chemistry, Tokyo Institute of Technology at Nagatsuta,
Nagatsuta-cho, Midori-ku, Yokohama 227

(Received June 15, 1983)

The structures of mono(glycinato)nickel(II) and tris(glycinato)nickelate(II) complexes in aqueous solution were determined by the X-ray diffraction method. From the analysis of the radial distribution curve of solution A, in which the hexaaqua- and mono(glycinato)nickel(II) ions coexisted (the mole ratio $C_{\mathrm{gly}}/C_{\mathrm{Ni}}=0.792$, where C_i denotes the total concentration of species i), we found that the mono(glycinato)nickel(II) complex combined with four water molecules at the distance of (2.08±0.01) Å, the bond being longer than the Ni–OH$_2$ bond (2.04 Å) within the $[\mathrm{Ni(OH_2)_6}]^{2+}$ ion. The Ni–O and Ni–N bond lengths within the mono(glycinato)nickel(II) complex were essentially the same and (2.09±0.02) Å. Therefore, the mono(glycinato)nickel(II) ion has a practically regular octahedral structure. The nonbonding Ni···C distance was also determined to be (2.87±0.02) Å. The X-ray scattering data of solutions having the $C_{\mathrm{gly}}/C_{\mathrm{Ni}}$ mole ratio of 3.24 (solution B) and 3.94 (solution C), in both of which almost all nickel(II) ions formed the $[\mathrm{Ni(gly)_3}]^-$ complex, showed that the tris(glycinato)nickelate(II) complex had a slightly distorted octahedral structure with the Ni–O and Ni–N bond lengths of (2.03±0.01) Å and (2.14±0.01) Å, respectively. The nonbonding Ni···C(COO), Ni···C(CH$_2$) and Ni···O(O=C) distances were (2.82±0.02) Å, (2.96±0.02) Å, and (4.07±0.03) Å, respectively.

Structures of chelate compounds of some transition metal ions were first determined for ethylenediamine complexes in aqueous solutions.[1–4] The chelate effect on the formation of the ethylenediamine complexes was discussed in connection with the structural data of the complexes determined by the X-ray diffraction experiments by comparing them with the structures of ammine complexes of the relevant metal ions.[5]

A large number of crystallographic data have been accumulated for aminocarboxylato complexes.[6] However, compounds so far studied by the X-ray crystallography were mostly non-charged ones, which were relatively easy to prepare single crystals. Therefore, usually the structure of only one compound has been known in a series of compounds of a metal ion having one kind but different numbers of ligands. In X-ray analysis of solutions a restriction of preparing a single crystal is eliminated, although another restriction for solubility of compounds may be introduced, instead.

Glycine is one of the most interesting and important compounds among chelating reagents. It is the most fundamental unit in the formation of proteins. Some metal ions, which react as catalysts in biochemical reactions, are often combined with amino acid residues within proteins. Therefore, structural data of aminocarboxylato complexes must be very important in elucidating mechanisms of biochemical reactions.

In the present study we aimed at determining the structures of the mono(glycinato)nickel(II) and tris(glycinato)nickelate(II) complexes in aqueous solution by the X-ray diffraction method. The bis(glycinato)nickel(II) complex is not soluble enough to determine the structure in an aqueous solution; instead, the structure has been determined in crystal.[7]

Experimental

Preparation and Analysis of Sample Solutions. All chemicals used were of reagent grade. Since it was difficult to achieve a high value of the average ligand number of the nickel(II)–glycine solutions by adding glycine to a nickel(II) salt solution at a high pH, we mixed diaquabis(glycinato)nickel(II) with sodium glycinate in water at a suitable pH for preparing solutions in which the tris(glycinato)nickelate(II) complex formed as the main species (solutions B and C). A solution of a relatively low ligand number, in which the mono(glycinato)nickel(II) complex was formed as a predominant species, was prepared by mixing a nickel(II) nitrate solution with crystals of the bis(glycinato)nickel(II) complex (solution A).

Bis(glycinato)nickel(II) was prepared by dissolving freshly precipitated nickel(II) carbonate to an aqueous glycine solution, and then recrystallized from water. *Sodium glycinate* was obtained by mixing sodium hydroxide and glycine in methanol and then recrystallized from methanol. *Nickel(II) nitrate* of reagent grade was recrystallized from water.

The total concentration of nickel(II) ions (C_{Ni}) in the sample solutions was gravimetrically determined as bis(dimethylglyoximato)nickel(II). The total glycine concentration (C_{gly}) of the solutions was determined by the Kjeldahl method. Concentrations of nitrate ions in solution A and of sodium ions in solutions B and C were estimated from the material balance of ions in the solutions. Densities of the sample solutions were measured pycnometrically. The composition of the solutions is given in Table. 1.

X-Ray Scattering Measurements. X-Ray scattering measurements were carried out with a JEOL θ-θ diffractometer by using

Table 1. The composition (mol dm^{-3}) and stoichiometric volume V per nickel atom in the solutions

	A	B	C
Ni	2.904	1.654	1.759
Na	—	2.056	3.411
O	60.62	51.60	50.00
N	5.808	5.364	6.929
C	4.602	10.73	13.68
H	100.2	103.2	100.0
V/Å^3	571.8	1004	944.0
$C_{\mathrm{gly}}/C_{\mathrm{Ni}}$	0.792	3.24	3.94
$C_{\mathrm{H_2O}}/C_{\mathrm{Na}}$	—	19.9	10.6
Density/g cm^{-3}	1.378	1.278	1.346

Mo *Ka* radiation (λ=0.7107 Å) in a room thermostated at (25±1) °C. The accessible range of scattering angle (2θ) was 2—140°. Times requiring to accumulate 120000 counts were recorded at each angle of measurements. The method of measurements and data treatments were described in previous papers.[1-5,8,9] All calculations were performed by using programs KURVLR[10] and NLPLSQ.[11] Computers at the Tokyo Institute of Technology was mainly used, but a part of the computation was carried out at the Institute for Molecular Science in Okazaki.

Results and Discussion

According to the stability constants of nickel(II)–glycine complexes[12] and the low solubility of the bis(glycinato)nickel(II) (about 0.12 mol dm^{-3}) so far reported in the literature, we can expect that comparable amounts of $[Ni(OH_2)_6]^{2+}$ and $[Ni(gly)]^+$ ions coexist in solution A, while almost all nickel(II) ions are present as the $[Ni(gly)_3]^-$ complex in solutions B and C. In solution B the concentration of sodium ions is smaller than that in solution C, and therefore, the C_{H_2O}/C_{Na} ratio in the former solution is about a double of that in the latter (see Table 1).

The observed $s \cdot i(s)$ and $D(r)$ curves of the solutions are shown in Figs. 1 and 2, respectively.

The structure of glycine has been determined crystallographically.[13,14] Since the intramolecular bond lengths within the glycinate ion in the bis(glycinato)nickel(II) are essentially the same as those in glycine, we assumed that the intramolecular bond distances within the glycinate ions coordinated to the central nickel(II) ion were independent of the complexes and the same as those reported in the literature.[7,13,14] The parameter values of water molecule, glycinate and nitrate ions used for the computations are summarized in Table 2. The numbering of the atoms within the glycinate ion coordinated to the nickel(II) ion is shown in Fig. 3.

Solution A. According to the stability constants of the nickel(II)–glycine complexes in the literature,[12] approximately the same amounts of $[Ni(OH_2)_6]^{2+}$ and $[Ni(gly)]^+$ ions may be formed in this solution. However, it should be noted that the stability constants determined in relatively dilute solutions may not be correctly applicable to calculations of distributions of the $[Ni(OH_2)_6]^{2+}$ and $[Ni(gly)]^+$ complexes in a concentrated solution like the sample solution in the present study.

The radial distribution curve of solution A is given in Fig. 2A. Figure 4 also represents the $D(r)$ function and the differential radical distribution curve, $D(r)-4\pi r^2\rho_0$, of solution A, where ρ_0 denotes the average scattering density in the stoichiometric volume V of the solution per Ni atom, as well as theoretical peak shapes of each atom pair in the system, for which we will discuss in the following section.

The broad and small peak around 1.3 Å observed in the $D(r)$ and $D(r)-4\pi r^2\rho_0$ curves (Fig. 4, a and e, respectively) is due to the O–H bonds within water molecules, the N–O bonds within nitrate ions and the N–H, C–H, C_1–C_2, C_2–N, $C_1\overset{\cdots}{-}O_1$, and $C_1\overset{\cdots}{-}O_2$ bonds within glycinate ions. The second peak at 2.1 Å is attributed to interactions between nickel and ligand atoms in the first coordination shell of the complexes. Nonbonding $C_1\cdots N$, $C_2\cdots O_1$, $C_2\cdots O_2$, and $O_1\cdots O_2$

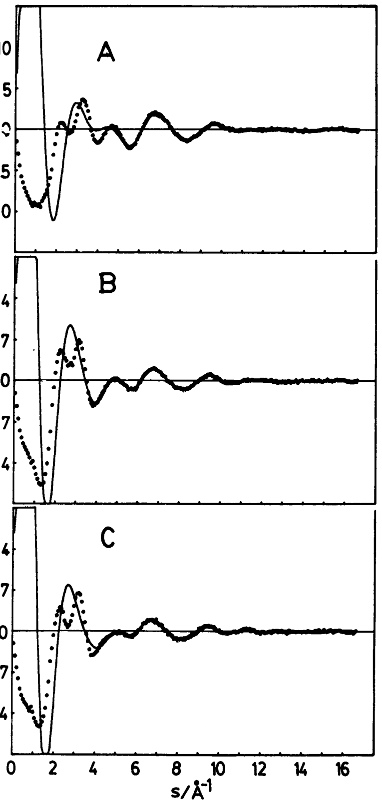

Fig. 1. The reduced intensities multiplied by s for solutions A, B, and C. The observed $s \cdot i(s)$ curves are shown by circles and calculated ones using parameter values finally obtained by solid lines.

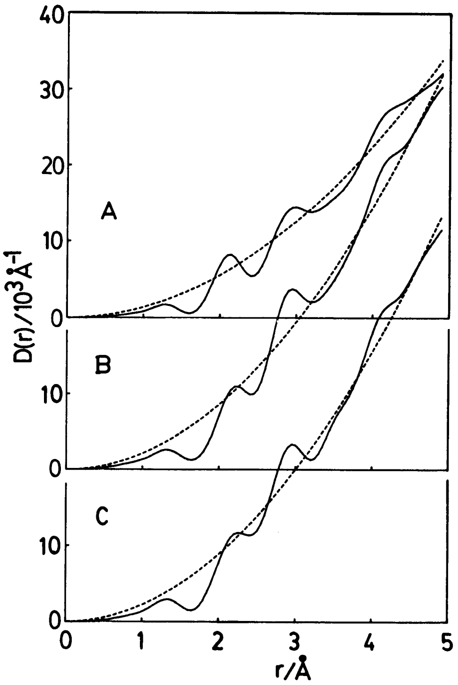

Fig. 2. The radial distribution curves, $D(r)$, for solutions A, B, and C. The dashed lines show the curve of $4\pi r^2\rho_0$.

Table 2. The bond distances (r) and temperature factors (b) for water molecule, glycinate, and nitrate ions

		r/Å	b/Å^2
H_2O	O–H	0.955$^{a)}$	0.010$^{a)}$
gly$^-$	C–H	1.09$^{b)}$	0.003$^{c)}$
	N–H	1.04$^{b)}$	0.003$^{c)}$
	C–C	1.52$^{b)}$	0.001$^{c)}$
	C–N	1.47$^{b)}$	0.001$^{c)}$
	$C\overset{\cdots}{-}O$	1.26$^{b)}$	0.001$^{c)}$
	C⋯N	2.48$^{b)}$	0.003$^{d)}$
	C⋯O	2.38$^{b)}$	0.003$^{d)}$
	O⋯O	2.23$^{b)}$	0.003$^{d)}$
NO_3^-	N–O	1.26$^{e)}$	0.0009$^{f)}$
	O⋯O	2.19$^{e)}$	0.002$^{f)}$

a) R. Triolo and A. H. Narten, *J. Chem. Phys.*, **63**, 3624 (1975). b) Refs. 13 and 14. c) Calculated values from spectroscopic data quoted from R. A. Condrate and K. Nakamoto, *J. Chem. Phys.*, **42**, 2590 (1965). d) Estimated values; even if the values were changed from 0 002 to 0 004 Å^2, practically the same results were obtained. e) R. Caminiti, G. Licheri, G. Piccaluga, and G. Pinna, *J. Chem. Phys.*, **68**, 1967 (1978). f) Ref. 1.

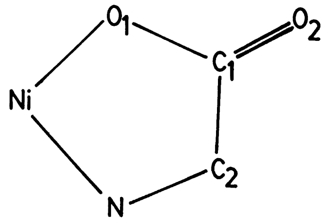

Fig. 3. The numbering of the atoms within the glycinate ion coordinated to the nickel(II) ion.

interactions within glycinate ions and O...O interactions within nitrate ions may also contribute, in part, to the peak (see Fig. 4, b—d). The third peak appearing at about 2.9 Å may be composed of peaks owing to nonbonding Ni⋯C$_1$ (and also Ni⋯C$_2$) pairs within the mono(glycinato)nickel(II) complex, interactions between the ligand atoms in the first coordination sphere of the complex, and to the O⋯O contacts in the bulk water.

The peak at 2.1 Å was well explained by assuming that all nickel atoms in the solution have six oxygen and nitrogen atoms in the first coordination sphere, independent of the concentration ratio of the $[Ni(OH_2)_6]^{2+}$ to $[Ni(gly)]^+$ ions. Since the Ni–O$_1$ and Ni–N bonds are hardly distinguishable by the X-ray diffraction analysis as previously pointed out,$^{3)}$ the result suggests that all nickel(II) ion in the solution have six ligand atoms and thus the $[Ni(gly)]^+$ complex should have additional four oxygen atoms in its first coordination sphere at the distance of about 2.1 Å. Therefore, we can conclude that the mono(glycinato)nickel(II) complex is described as $[Ni(gly)(OH_2)_4]^+$ and has an almost regular octahedral structure.

In order to refine the structural parameters of the mono(glycinato)nickel(II) ion in the solution, we first assumed that concentrations of both the $[Ni(OH_2)_6]^{2+}$ and $[Ni(gly)(OH_2)_4]^+$ ions are 50 mol%, and the least-squares method was employed to the refinement of the structural parameters of the $[Ni(gly)(OH_2)_4]^+$ ion at the fixed composition of the solution. In this calculation the structural parameters of the $[Ni(OH_2)_6]^{2+}$ ion were quoted from the work by Ohtaki *et al.*$^{15)}$ and fixed at the literature values. The structural parameters of the bulk water were taken from the work by Narten.$^{16)}$

Table 3. Results of the least-squares refinements of solution A

Parameter values refined were bond distances (r/Å) and temperature factors (b/Å^2). Standard deviations are given in parentheses.

Interaction	Parameter	A-I (s>4.5 Å^{-1})	A-II (s>7.0 Å^{-1})
Ni–OH_2	r	2.08 (1)	2.08 (1)
	b	0.0052 (3)	0.0044 (2)
OH_2⋯OH_2	r	2.94$^{a)}$	2.94$^{a)}$
	b	0.012 (2)	0.009 (2)
Ni–O$_1$ Ni–N	r	2.09 (2)	2.09 (2)
	b	0.006 (1)	0.005 (1)
OH_2⋯O$_1$ OH_2⋯N	r	2.94$^{a)}$	2.94$^{a)}$
	b	0.010$^{a)}$	0.010$^{a)}$
N⋯O$_1$	r	2.87$^{a)}$	2.87$^{a)}$
	b	0.010$^{a)}$	0.010$^{a)}$
Ni⋯C$_1$ Ni⋯C$_2$	r	2.87 (2)	2.82 (2)
	b	0.008 (1)	0.005 (1)

a) The values were kept constant during the calculation.

Two types of the least-squares method were carried out in the present case (Table 3). In the A-I type calculation, the intensity data in the range $s>4.5$ Å^{-1} were used and the contribution of the O⋯O contacts in the bulk water was taken into account in the course of the refinement. On the other hand, in the A-II calculation the O⋯O interactions in the bulk water were not taken into consideration, and the intensity data used for the calculation were those in the range $s>7.0$ Å^{-1}, where the long-range interactions did not significantly contribute to the calculation. Since oxygen and nitrogen atoms have similar scattering factors over the whole angle range, the lengths of the Ni–O$_1$ and Ni–N bonds were not determined separately with reasonable certainties by the least-squares method. Therefore, we assumed that the Ni–O$_1$ and Ni–N bonds have the same structural parameters in the present stage of calculations. The results obtained by the A-I and A-II type calculations were very similar (see Table 3), and thus the Ni–OH_2 bond length within the $[Ni(gly)(OH_2)_4]^+$ complex was determined to be 2.08 Å and the lengths of the Ni–O$_1$ and Ni–N bonds were estimated to be 2.09 Å. Even if we changed the concentration ratio of $[Ni(OH_2)_6]^{2+}$ to $[Ni(gly)(OH_2)_4]^+$ from 30 : 70 to 70 : 30, no significant improvement of the result was achieved under the present assumption of the same length of the Ni–O$_1$ and Ni–N bonds.

A possibility of different lengths of the Ni–O$_1$ and Ni–N bonds may not still be well eliminated by the above calculation, because the initial values, in which the Ni–O$_1$ and Ni–N bonds are assumed to have the same length, may give a very shallow minimum of the error-square sum in the course of the least-squares refinement of the structural parameters and the parameter values may not be well floated to reach a set of the best values. Therefore, at the next step of the refinement of the result, we stepwise changed the initial values of the lengths of the Ni–O$_1$ and Ni–N bonds, as well as the mole ratio of $[Ni(OH_2)_6]^{2+}$ to $[Ni(gly)(OH_2)_4]^+$. In this case, we assumed that the Ni–OH$_2$ bond was 2.08 Å and the temperature factor of the bond was stepwise changed from 0.003 Å^2 to 0.006 Å^2. The temperature factors of the Ni–O$_1$ and Ni–N bonds were fixed at 0.003 Å^2, which was found from the analysis of the structure of the tris(glycinato)nickelate(II) complex in solutions B and C, as will be described in the later section. Although the value was smaller than that estimated from the least-squares method in Table 3, we considered that the temperature factor of 0.003 Å^2 for the Ni–O$_1$ and Ni–N bonds was more reliable one than 0.005—0.006 Å^2 in Table 3, because the former value of the temperature factor was determined in solutions B and C in which the $[Ni(gly)_3]^-$ complex existed as the main species and the structure of the complex was more accurately analyzed than that of the $[Ni(gly)(OH_2)_4]^+$ complex coexisting with $[Ni(OH_2)_6]^{2+}$. Moreover, we can expect that the temperature factors of the Ni–O$_1$ and Ni–N bonds within the $[Ni(gly)(OH_2)_4]^+$ complex may not be greatly different from those within the $[Ni(gly)_3]^-$ ion.

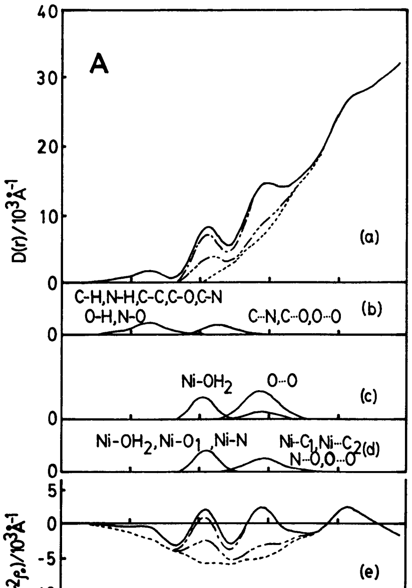

Fig. 4. (a) The radial distribution curve for solution A. (b) The theoretical peaks for O–H bonds within water molecule, intramolecular interactions within glycinate ion, and N–O and O···O pairs within nitrate ion. (c) The theoretical peak shapes calculated for Ni–OH$_2$ and O···O pairs within the hexaaquanickel(II) complex and O···O contacts of water molecules in the bulk. (d) The theoretical peak shapes owing to Ni–OH$_2$, Ni–O$_1$, Ni–N, Ni···C$_{1,2}$, N···O, and O···O pairs within the mono-complex. (e) The corresponding $(D(r)-4\pi r^2\rho_0)$ curve to the $D(r)$ in (a). The chain, double chain and dashed lines show the residual curves after subtraction of the theoretical peaks in (b), (c), and (d), respectively.

In the course of the refinement of the structural parameters of the $[Ni(gly)(OH_2)_4]^+$ ion, we extracted the second peak of the radial distribution curve given in Fig. 2A. By subtracting intramolecular interactions of water molecules, glycinate and nitrate ions, we can obtain the radial distribution curve which contains the only peaks ascribed to interatomic distances within the complexes around 2.1 Å and to longer range interatomic interactions in the region of larger r values. The peak at about 2.1 Å (the second peak in the original $D(r)$ curve) was extracted from the residual radial distribution curve by assuming a symmetrical shape of approximately Gaussian (Fig. 5). Since we could expect that the peak consisted of peaks owing to the Ni–OH$_2$ bonds within the $[Ni(OH_2)_6]^{2+}$ ion, Ni–OH$_2$, Ni–O$_1$, and Ni–N bonds within the $[Ni(gly)(OH_2)_4]^+$ complex, the refinement of the structural parameters of the $[Ni(gly)(OH_2)_4]^+$ ion was carried out in order to minimize the error-square sum defined by Eq. 1 at various sets of the temperature factor of the Ni–OH$_2$ bond, lengths of the Ni–O$_1$ and Ni–N bonds and the mole ratio of $[Ni(OH_2)_6]^{2+}$ to $[Ni(gly)(OH_2)_4]^+$.

$$U = \sum w\{D(r)^{\mathrm{2nd\ peak}}_{\mathrm{calcd}} - D(r)^{\mathrm{2nd\ peak}}_{\mathrm{obsd}}\}^2 \tag{1}$$

Here $D(r)^{\mathrm{2nd\ peak}}$ denotes the $D(r)$ values at the second peak of the radial distribution curve extracted from the original curve by the procedure mentioned above. w is given as $\exp(-\alpha\cdot\Delta l^2)$, where $\Delta l = r_0 - r$ and r_0 represents the r-value at the center of the second peak. In this calculation we assumed that the r_0 value was 2.08 Å. The value α was estimated from the half-width of the second peak extracted.

In the course of the present calculations we fixed the values of all the structural parameters of the $[Ni(OH_2)_6]^{2+}$ ion at the literature values,[15] as well as the length of the Ni–OH$_2$ bond at 2.08 Å and the temperature factors of the Ni–O$_1$ and Ni–N bonds at 0.003 Å^2.

The minimum error-square sum was obtained for the set in which the temperature factor of the Ni–OH$_2$ bond within the $[Ni(gly)(OH_2)_4]^+$ was 0.003 Å^2. In Table 4 are summarized values of the error-square sums for various sets of the lengths of the Ni–O$_1$ and Ni–N bonds and the mole ratio of $[Ni(OH_2)_6]^{2+}$ to $[Ni(gly)(OH_2)_4]^+$.

TABLE 4. RESULT OF THE ANALYSIS OF THE SECOND PEAK IN THE $D(r)$ CURVE OF SOLUTION A

Error-square sums ($U\times10^{-5}$/Å^{-2}) were calculated according to the equation in the text. The Ni–OH$_2$ bond distance and all the temperature factors within the mono-complex were kept constant at 2.08 Å and 0.003 Å^2, respectively, in the course of the calculation.

		Mole fraction				
	Ni^{2+} =	0.3	0.4	0.5	0.6	0.7
	$Ni(gly)^+$ =	0.7	0.6	0.5	0.4	0.3
Bond distance r/Å		$U\times10^{-5}$/Å^{-2}				
Ni–O$_1$ Ni–N	2.05 2.13	4.7	4.3	5.0	6.7	9.3
Ni–O$_1$ Ni–N	2.07 2.11	4.6	4.1	4.7	6.4	9.0
Ni–O$_1$ Ni–N	2.09 2.09	4.5	*4.0*	4.6	6.2	8.8

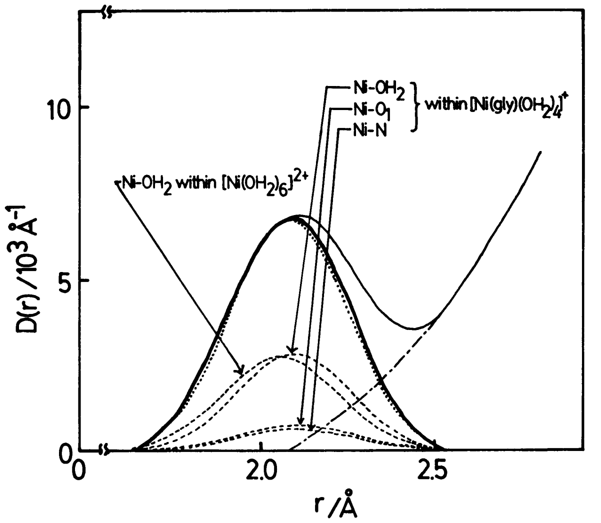

Fig. 5. The second peak of the radial distribution curve for solution A. The thin and thick solid lines represent the experimental and extracted $D(r)$ curves, respectively, and the chain line indicates the residual curve after extraction. The theoretical peak shapes owing to the $Ni-OH_2$ bonds within the $[Ni(OH_2)_6]^{2+}$ ion and $Ni-OH_2$, $Ni-O_1$, and Ni–N bonds within the $[Ni(gly)(OH_2)_4]^+$ ion are shown by dashed lines. The dotted line represents the peak shape by summing up ones shown by dashed lines.

$(OH_2)_4]^+$ at the value of 0.003 $Å^2$ for the temperature factor of the $Ni-OH_2$ bond.

In Fig. 5 was shown the coincidence of the experimentally obtained curve (the peak extracted by the procedure described previously) with the calculated shape by summing up shapes owing to the $Ni-OH_2$ interactions within the $[Ni(OH_2)_6]^{2+}$ ion and to the $Ni-OH_2$, $Ni-O_1$, and Ni–N bonds within the $[Ni(gly)(OH_2)_4]^+$ complex.

From the result we concluded that the $Ni-O_1$ and Ni–N bonds within the $[Ni(gly)(OH_2)_4]^+$ have practically the same length of 2.09 Å and thus the $[Ni(gly)(OH_2)_4]^+$ complex is essentially regular octahedral. The mole ratio of the $[Ni(OH_2)_6]^{2+}$ to the $[Ni(gly)(OH_2)_4]^+$ ions was approximately 40 : 60 in the present solution.

Solutions B and C. In solutions B and C, the tris(glycinato)nickelate(II) complex may be present as the main species. The radial distribution curves obtained for solutions B and C are shown in Fig. 2. They are very similar in shape, but it should be noted that the radial distribution curve of solution C has a small hump at about 3.4 Å, the concentration of sodium ions in solution C being higher than in solution B.

The radial ($D(r)$) and differential radial ($D(r)-4\pi r^2\rho_0$) distribution curves are shown in Fig. 6, a and e, respectively, for solution B. In the curves we see four peaks at 1.3, 2.2, 3.0, and 4.0 Å.

The peak at 1.3 Å can be ascribed to the O–H bonds within water molecules and N–H, C–H, C_1-C_2, C_2-N, $C_1\overset{...}{-}O_1$, and $C_1\overset{...}{-}O_2$ bonds within glycinate ions. The second peak consists mainly of interactions between nickel atoms and oxygen and nitrogen atoms within the glycinate ions coordinated. Nonbonding $C_1\cdots N$, $C_2\cdots O_1$, $C_2\cdots O_2$, and $O_1\cdots O_2$ interactions within glycinate ions also contribute, in part, to the peak. The Na–O pairs within the hydrated sodium ions should have the bond length of about 2.4 Å,[17] which might also appear in this region in the $D(r)$ curve. The third peak may be composed of peaks due to nonbonding interactions between nickel and carbon atoms of the carboxylato and methylene groups within the glycinate ions coordinated, between ligand atoms in the coordination sphere of the $[Ni(gly)_3]^-$ complex, and between oxygen atoms in the bulk water. In the fourth peak at about 4 Å, nonbonding $Ni\cdots O_2$ and other long-range interactions may be included.

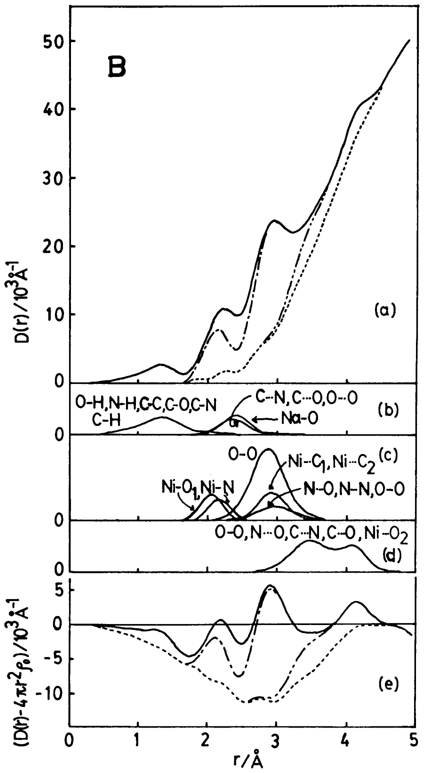

Fig. 6. (a) The radial distribution curve for solution B. (b) The theoretical peak shapes calculated for the O–H bonds within water molecule, the intramolecular interactions within glycinate ion, and Na–O pairs within hydrated sodium ion. (c) The theoretical peaks for $Ni-O_1$, Ni–N, $Ni\cdots C_{1,2}$, $N\cdots O$, $N\cdots N$, and $O\cdots O$ pairs within the tris-complex and $O\cdots O$ contacts of water molecules in the bulk. (d) The theoretical peaks for $O\cdots O$ contacts within hydrated sodium ion and $Ni\cdots O_2$, $N\cdots O_2$, $C_{1,2}\cdots N$, and $C_{1,2}\cdots O_1$ pairs within the tris-complex. (e) The corresponding ($D(r)-4\pi r^2\rho_0$) curve to the $D(r)$ in (a). The chain, double chain, and dashed lines indicate the residual curves after subtraction of the theoretical peaks in (b), (c), and (d), respectively.

As we have pointed out in the previous section, we found a small hump at about 3.4 Å in the radial distribution curve of solution C, in which a higher concentration of sodium ions was contained than in solution B. This fact suggests that the hump may be due to interactions within hydrated sodium ions.

At the first step of analysis of the radial distribution curve of solution B, as well as that of solution C, we first subtracted peak shapes of known interatomic distances within glycinate ions and the bulk water (Fig. 6b). The interaction between sodium ion and water molecules hydrated must also be taken into account in the calculation.

The structure of hydrated sodium ion has been determined in solutions of relatively low[17] and high[18] concentrations. Caminiti *et al.*[17] showed that a sodium ion had six water molecules in the first coordination shell at the distance of 2.41 Å. Calculations by using molecular dynamics simulations for the structure of *ca.* 0.5—2 mol dm^{-3} aqueous solutions of sodium chloride led to the hydration number of about 6—8 for sodium ions.[18] On the other hand, Maeda and Ohtaki found that the hydration number of sodium ion was four in a 7 mol dm^{-3} NaI solution.[19] If sodium ion has six water molecules coordinated in the form of a regular octahedron, we can expect to find the nonbonding water–water distance within the hydrated sodium ion at about 3.4 Å ($=2.4$ Å$\times\sqrt{2}$). On the other hand, in the four-coordinated sodium ion with water molecules, the nonbonding water-water interactions within the hydration shell of the sodium ion may appear at about 3.9 Å ($=2.4$ Å$\times\sqrt{8/3}$).

If we assumed the tetrahedral structure of the hydrated sodium ion in the solution and subtracted the intramolecular interactions within the hydrated ion from the radial distribution function, a peak remained at about 3.4 Å in the $D(r)$ curve of both solutions B and C, which was not satisfactorily explainable by possible atom pairs in the system. However, when the octahedral structure was assumed for the hydrated sodium ion, the radial distribution curves of both solutions B and C were well interpreted in terms of peak shapes of all the possible combinations of atom pairs shorter than 4 Å, as will be described in more detail in the later section.

Thus, we concluded that sodium ion has six water molecules at the distance of 2.40 Å in such solutions of relatively low concentrations as those in the present case.

When we subtracted the peak shapes of the Na–O interactions within the hexa-hydrated sodium ions and intramolecular bonding and nonbonding interactions within glycinate ions and water molecules (see Fig. 6b), we found a peak remaining at about 2.1 Å. The peak must be ascribed to the Ni–O_1 and Ni–N interactions within the $[Ni(gly)_3]^-$ complex. The shape of the peak was quite symmetrical. However, it was difficult to reproduce the peak shape by a single Gaussian curve which was constructed from the Ni–O_1 and Ni–N bonds with the same length, because the temperature factor of the bonds become unreasonably large (0.01—0.02 $Å^2$). Therefore, we assumed that the peak at 2.1 Å consisted of two peaks of Ni–O_1 and Ni–N bonds with different lengths. By a trial-and-error method the peak was separated into two, one had the peak position at 2.04 Å and the other was centered at 2.15 Å; the value of the temperature factors of the both bonds seemed to be reasonable ($\simeq$0.003 $Å^2$).

It is not straightforward to identify which peak corresponds to the Ni–O_1 or Ni–N bond. It has been found in crystal of *fac*-$[Cr(gly)_3]\cdot H_2O$ that the metal-oxygen bond is shorter than the metal-nitrogen bond within the complex.[20] The fact that the metal-oxygen bond is shorter than the metal-nitrogen bond has been found by many crystallographic investigations of various glycinato complexes. When we make a model structure of the $[Ni(gly)_3]^-$ ion by using three glycinate ions and one nickel(II) ion of an ionic radius of about 0.69 Å,[21] the glycinate ions are largely deformed and strained if we assume that the Ni–O_1 bond is longer than the Ni–N bond. On the other hand, the structural model having the Ni–O_1 bond of about 2.04 Å and the Ni–N bond of about 2.15 Å shows no large deformation in the bond angles within the glycinate ions. Therefore, we concluded that the peak at 2.04 Å is attributed to the Ni–O_1 bond, while the other peak at 2.15 Å is ascribed to the Ni–N bond within the tris(glycinato)-nickelate(II) complex.

The structural parameters of the tris(glycinato)-nickelate(II) complex were finally refined by the least-squares method by inserting the values for each interatomic interaction estimated by the trial-and-error method previously described as the initial values. The least-squares refinement of the structural parameters of the $[Ni(gly)_3]^-$ ion was performed by using $s\cdot i(s)$ data over the range $s>4$ $Å^{-1}$. In the refinement three types of calculations were carried out on slightly different assumptions.

In the B-I calculation all the distances and the temperature factors listed in Table 5 were refined by

TABLE 5. RESULTS OF THE LEAST-SQUARES REFINEMENTS OF SOLUTION B

Parameter values refined were bond distances (r/Å), temperature factors (b/$Å^2$), and frequency factors (n). Standard deviations are given in parentheses.

Interaction	Parameter	B-I	B-II	B-III
Ni–O_1	r	2.039 (4)	2.034 (4)	2.031 (4)
	b	0.0032 (2)	0.0031 (2)	0.0031 (2)
	n	3.0[a]	3.0[a]	3.2 (1)
Ni–N	r	2.153 (5)	2.154 (5)	2.162 (5)
	b	0.0032 (3)	0.0031 (3)	0.0032 (2)
	n	3.0[a]	3.0[a]	3.3 (1)
N···O_1	r	2.80 (6)	2.76[a]	2.76[a]
	b	0.006 (3)	0.006[a]	0.006[a]
O···O	r	2.98 (7)	2.96[a]	2.96[a]
	b	0.006 (3)	0.006[a]	0.006[a]
N···O	r	3.01 (7)	2.97[a]	2.97[a]
	b	0.006 (3)	0.006[a]	0.006[a]
N···N	r	3.21 (9)	3.21[a]	3.21[a]
	b	0.006 (3)	0.006[a]	0.006[a]
Ni···C_1	r	2.82 (1)	2.83 (1)	2.82 (2)
	b	0.008 (1)	0.008 (1)	0.009 (1)
	n	3.0[a]	3.0[a]	3.0 (1)
Ni···C_2	r	2.97 (1)	2.98 (1)	2.98 (2)
	b	0.008 (1)	0.008 (1)	0.009 (1)
	n	3.0[a]	3.0[a]	3.1 (1)
Ni···O_2	r	4.08 (2)	4.09 (2)	4.09 (2)
	b	0.006 (1)	0.007 (1)	0.007 (1)
	n	3.0[a]	3.0[a]	3.2 (1)

a) The values were kept constant during the calculation.

Table 6. Bond lengths (r/Å) within the tris(glycinato)nickelate(II) complexes found in solutions B and C

Interaction	Solution B	Solution C	Proposed value
Ni–O_1	2.039±0.004	2.019±0.004	2.03±0.01
Ni–N	2.153±0.005	2.133±0.005	2.14±0.01
Ni···C_1	2.82±0.01	2.82±0.01	2.82±0.02
Ni···C_2	2.97±0.01	2.95±0 01	2.96±0 02
Ni···O_2	4.08±0.02	4.06±0.02	4.07±0.03

Table 7. Nickel(II)–ligand bond lengths (r/Å) in the hydrated nickel ion and glycinato–nickel(II) complexes

Complex	Ni–OH_2	Ni–O_1	Ni–N
$[Ni(OH_2)_6]^{2+}$ [a]	2.04	—	—
$[Ni(gly)_2(OH_2)_4]^+$	2.08	2.09	2.09
$[Ni(gly)(OH_2)_2]$ [b]	2.10	2.06	2.08
$[Ni(gly)_3]^-$	—	2 03	2.14

a) Ref. 15. b) Ref. 7.

keeping all the frequency factors constant. In the B-II treatment some interatomic interactions of relatively long distances were allowed to remain unchanged. The B-III calculation was carried out on similar assumptions given at the B-II calculation except for the frequency factors of some atom-pairs floated in the course of the refinement. All the calculations gave quite similar results, and we adopted the values obtained by the B-I type calculation as the final ones for the tris(glycinato)-nickelate(II) complex in solution B.

In the course of the calculation the existence of the *fac*- and *mer*-isomers of the tris(glycinato)nickelate(II) complex was taken into account. However, since the difference between the isomers was so small, the introduction of the existence of the isomers did not improve the result.

For solution C a similar procedure of calculations were performed to obtain the structural parameters of the tris(glycinato)nickelate(II) complex in the solution in order to examine reproducibility of the result. The interatomic distances found for the $[Ni(gly)_3]^-$ complex in solution C are listed in Table 6, together with those obtained in solution B. The proposed values of the bond lengths within the tris(glycinato)nickelate(II) complex are also given in the table.

In Table 7 we summarized the lengths of the Ni–OH_2, Ni–O_1, and Ni–N bonds within the hexaaqua-, tetraaquamono(glycinato)- and diaquabis(glycinato)nickel(II) and tris(glycinato)nickelate(II) complexes.

It can be noted that the Ni–OH_2 distance increases with the increased number of glycinate ions coordinated. The same trend may be seen for the Ni–N bond. On the contrary, the Ni–O_1 distance decreases with the increase in the number of glycinate ions in the coordination sphere of nickel(II) ion. The result suggests that the electrostatic interaction between the central nickel (II) ion and a charged donor atom is enhanced, while the coordination interaction between the metal ion and an uncharged donor atom weakens.

The work has been financially supported, in part, by the Grant-in-Aid for Scientific Research No. 57470054 from the Ministry of Education, Science and Culture. The financial aid by the Asahi Glass Foundation for Industrial Technology is also acknowledged. A part of the computer calculations carried out in the present work has been performed at the Institute for Molecular Science in Okazaki.

References

1) T. Fujita, T. Yamaguchi, and H. Ohtaki, *Bull. Chem. Soc. Jpn.*, **52**, 3539 (1979).

2) T. Fujita and H. Ohtaki, *Bull. Chem. Soc. Jpn.*, **53**, 930 (1980).

3) T. Fujita and H. Ohtaki, *Bull. Chem. Soc. Jpn.*, **55**, 455 (1982).

4) T. Fujita and H. Ohtaki, *Bull. Chem. Soc. Jpn.*, **56**, 3276 (1983).

5) H. Ohtaki, "Advances in Solution Chemistry," ed by I. Bertini, L. Lunazzi, and A. Dei, Plenum, New York (1981), p. 67.

6) H. C. Freeman, *Adv. Protein Chem.*, **22**, 258 (1967).

7) H. C. Freeman and J. M. Guss, *Acta Crystallogr., Sect. B*, **24**, 1133 (1968).

8) H. Ohtaki and M. Maeda, *Bull. Chem. Soc. Jpn.*, **47**, 2194 (1974); H. Ohtaki, M. Maeda, and S. Ito, *Bull. Chem. Soc. Jpn.*, **47**, 2217 (1974).

9) T. Yamaguchi and H. Ohtaki, *Bull. Chem. Soc. Jpn.*, **51**, 3227 (1978).

10) G. Johansson and M. Sandström, *Chem. Scr.*, **4**, 195 (1973).

11) T. Yamaguchi, Doctor Thesis, Tokyo Institute of Technology, March (1978).

12) A. E. Martell and R. M. Smith, "Critical Stability Constants," Plenum, New York (1974), Vol. 1.

13) R. E. Marsh, *Acta Crystallogr.*, **11**, 654 (1958).

14) L. F. Power and K. E. Turner, *Acta Crystallogr., Sect. B*, **32**, 11 (1976).

15) H. Ohtaki, T. Yamaguchi, and M. Maeda, *Bull. Chem. Soc. Jpn.*, **49**, 701 (1976).

16) A. H. Narten, *ORNL*-**4578** (1970).

17) R. Caminiti, G. Licheri, G. Piccaluga, and G. Pinna, *Rend. Sem. Fac. Sci. Univ. Cagliari*, **47**, 1 (1977).

18) K. Heinzinger and P. C. Vogel, *Z. Naturforsch., A*, **31**, 463, 476 (1976).

19) M. Maeda and H. Ohtaki, *Bull. Chem. Soc. Jpn.*, **48**, 3755 (1975).

20) R. F. Bryan, P. T. Greene, P. F. Stckely, and E. W. Wilso, Jr., *Inorg. Chem.*, **10**, 1468 (1971).

21) R. D. Shannon, *Acta Crystallogr., Sect. A*, **32**, 751 (1976).